Very Large Infrared Two-Photon Absorption Cross Section of Asymmetric Zinc Porphyrin Aggregates: Role of Intermolecular Interaction and Donor−Acceptor Strengths

Paresh Chandra Ray* and Zuhail Sainudeen

Department of Chemistry, Jackson State University, Jackson, Mississippi 39217

Received: June 23, 2006; In Final Form: September 3, 2006

Very large two-photon absorption (TPA) cross sections at the infrared region have been revealed for J-aggregates of asymmetric zinc porphyrin using quantum-chemical calculation. The TPA properties are evaluated for monomer and aggregates of a series of push−pull porphyrins, whose syntheses are known in the literature. The two-photon absorption cross section can be greatly enhanced by increasing the strengths of the electron donor/acceptor. We also present a quantum-chemical analysis on porphyrin aggregates to understand the role of intermolecular interactions and the relationship between structural and collective nonlinear optical properties. It has been observed that the TPA properties change tremendously as monomers undergo J-aggregation and the magnitudes of TPA cross sections are highly dependent on the nature of aggregates. The importance of our results with respect to the design of photonic and photodynamic therapy materials has been discussed.

Introduction

Two-photon absorption (TPA) is defined as the electronic excitation of a molecule induced by a simultaneous absorption of a pair of photons of the same or different energy. In recent years, there has been growing interest in the design and synthesis of organic nonlinear optical materials[1−26] with large TPA cross section value because of their potential application in power limiting,[27] up-conversion lasing,[28] three-dimensional fluorescence imaging,[29] pulse reshaping and stabilization,[30] photodynamic therapy,[31−33] three-dimensional optical data storage,[34] and microfabrication.[35] Furthermore, they can be very useful in the production of memory devices. Current optical memory devices, which use a heat mode recording method to store information two-dimensionally, have a storage density limit of approximately gigabits per square centimeter. The creation of 3-D optical memory devices that use TPA materials and a photon mode recording method is expected to significantly increase the potential storage density to as high as terabits of information per cubic centimeter. This information density is the equivalent of $\sim 1 \times 10^6$ floppy disks, and the use of a TPA material would also result in an ultrafast access speed. The development of the two-photon technology depends much on the success of designing new molecules with large TPA cross sections at desirable wavelengths. It has been proposed that a molecular design that would result in a large TPA cross section ($\sigma^{(2)}$) would be composed of sets of terminal donor/acceptors interspersed with a π-conjugation system. Porphyrins and phthalocyanines are thus very likely candidates for 2PA materials because of their highly conjugated large π-system. However, monomeric metal-free porphyrins have shown only small $\sigma^{(2)}$ values, typically $\sim$10 GM where 1 GM = 10^{-50} cm^4 s molecule^{-1} photon^{-1}, when measured using femtosecond pulsed lasers. One of the key design strategies to enhance TPA properties is to modify the porphyrin ring by changing the metal atom in the center of the ring or by adding different donor (D) and acceptor (A) substituents at the ring. Another strategy would be to design the oligomers or aggregates of porphyrins. Several recent experimental observations[1,2,10−16] reported that $\sigma^{(2)}$ values can be enhanced by 2 orders of magnitudes by designing π-conjugated dimers. Drobizhev et al.[14] have found that a *meso*-butadiyne-linked symmetrical porphyrin dimer possesses an extremely large intrinsic (femtosecond) two-photon absorption cross section in the near-IR region. This corresponds to a factor of $\sim$400 of enhancement for the dimer as compared to the parent monomer, measured at the same wavelength. Collini et al.[10] have reported 30-fold enhancement of the σ_{TPA} value of H_4TPPS^{2-} in the range 400−440 nm when aggregation occurs. All the experimental data for dimer reported till now are for symmetric porphyhrin systems. To better understand the nature of this strong enhancement effect in aggregate systems and to elucidate the role of molecular structure, we present here a comprehensive study of two-photon absorption properties of a series of asymmetric porphyrin monomers, dimers, and aggregates (Scheme 1). Here, we have shown that the two-photon absorption can be observed at wavelengths from 1100 to 1700 nm, a range that spans the entire spectrum presently used in fiber telecommunications.

The study of TPA properties of porphyrins has been the focus of many recent works[31−33] because they are suitable candidates for the pharmaceutical industry because of their pronounced TPA in the infrared region, which can be exploited in the field of photodynamic therapy. One important potential application of this property would be in the treatment of cancer. Porphyrin derivatives are presently used as photosensitizers in one-photon PDT for cancer treatment. Photofrin (actually a mixture of porphyrins, including protoporphyrin, haematoporphyrin, and hydroxyethyldeuterioporphyrin), one of the two FDA-approved sensitizers, is usually irradiated at 630 nm, which limits the penetration of light through the tissue to just a few mm. Hence, the efficiency of the treatment is limited by the poor permeability of the surface tissue to the visible light used to irradiate the porphyrins. The maximum transmittance of skin tissue is in the 700−1500 nm region and the development of a PS with a maximum absorbance in this region remains a major challenge. The advantages of using light in these wavelength region are

* To whom correspondence should be addressed. E-mail: paresh.c.ray@ccaix.jsums.edu.

10.1021/jp063930z CCC: $33.50
Published on Web 10/13/2006

SCHEME 1: Structure of Tetrakis(4-sulfonatophenyl) Porphyrin

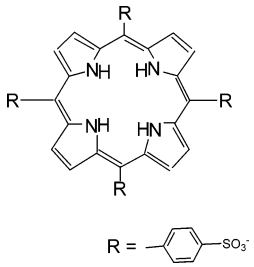

the ability to transmit through the silica fiber optic delivery systems and the deeper penetration in water (more than 100 μm). Thus, TPA-PDT may allow the localized treatment of cancer even at significant depths below the surface tissue. It is thus highly desirable to design and synthesize two-photon absorption materials acting at these fundamental wavelengths. In this paper, we have investigated theoretically the molecular designs of π-conjugated asymmetric porphyrin monomers, dimers, and aggregates possessing strong infrared two-photon absorption cross sections, which can be suitable candidates for TPA-PDT materials.

In this paper, we report a systematic study of the TPA properties of push−pull porphyrins using a combination of density functional theoretical (DFT) calculations with fairly extensive basis set [6-31G (d,p)] for geometry optimization and Zerner's intermediate neglect of differential overlap/correction vector (ZINDO/CV) method[20,36−43] properties calculations. Recently, we have shown that ZINDO/CV model allows obtaining complex first hyperpolarizabilities[36−42] and TPA[20,43] properties that can be directly compared with the outcome of the experimental measurements. To understand how the solvent polarity affects the structure of the porphyrin molecules, we have used self-consistent reaction field (SCRF) approach with polarizable continuum model (PCM).[44] To account for the solvent effects on TPA properties, we have adapted the ZINDO/CV technique with Onsager SCRF method.[45]

Computational Methods

Geometry optimizations were performed at the unrestricted Kohn−Sham level utilizing the Becke3 hybrid exchange functional combined with the Lee, Yang, and Parr correlation functional B3LYP as implemented in Gaussian03[46] package. The calculation has been performed with the 6-31G(*d*,p) basis set for carbon, hydrogen, and nitrogen. Effective core potentials and basis sets of Stevens et al.[47] were used for zinc. SCF calculations involve basis sets which include diffuse functions SCF = tight to request tight SCF convergence criteria. In all calculations, an ultrafine integration grid was used to ensure numerical accuracy. The optimized structure was used to calculate vibrational frequencies. Importantly, none of the frequency calculations generated negative frequencies; this is consistent with an energy minimum for the optimized geometry. To explicitly take into account the solvent polarity effects, we have adapted SCRF approach with the PCM[44] in its integral equation formalism (IEF) formulation as implemented in Gaussian 03.[46]

The TPA process corresponds to the simultaneous absorption of two photons. The TPA efficiency of an organic molecule, at optical frequency $\omega/2\pi$, can be characterized by the TPA cross sections $\delta(\omega)$. The TPA cross section is related to the imaginary part of the second hyperpolarizability $\gamma(-\omega;\omega,\omega,-\omega)$ by[19−26]

$$\delta(\omega) = \frac{3\hbar\omega^2}{2n^2c^2} L^4 \,\mathrm{Im}\langle\gamma(-\omega;\omega,\omega,-\omega)\rangle \qquad (1)$$

where $\hbar$ is Planck's constant divided by 2π, n is the refractive index of medium, c is the speed of light, and L is a local field factor (equal to 1 for vacuum). ZINDO/CV methodology is adopted here to calculate the second hyperpolarizabilities. Details about the methodology have been discussed in our recent publication.[20,36−43]

To account the solvent polarity effect in the ZINDO/CV approach, we have used expanded Onsager self-consistent reaction field (SCRF) theory[45] where self-consistent solute/solvent interactions are described by multipolar terms up to $l = 1-12$. According to this procedure, the reaction field R can be defined as

$$R = g_L(\epsilon)\langle\psi|M_{lm}|\psi\rangle \qquad (2)$$

where M_{lm} is the moment of the solute charge distribution and the proportional constant g is the modified Onsager factor that can be defined as

$$g_l(\epsilon) = \frac{1}{a^{2l+1}} \frac{(l+1)(\epsilon-1)}{l+\epsilon(l+1)} \qquad (3)$$

for $l = 1$ (dipolar term)

$$g(\epsilon) = \frac{2(\epsilon-1)}{(2\epsilon+1)a_0^3} \qquad (4)$$

where ϵ is the dielectric constant of the solvent and a_0 is the radius of the spherical cavity.

In this study, we first optimized the geometry at the DFT/PCM level in the presence of appropriate dielectric for different solvents using the Gaussian-03 package. The optimized DFT level geometry is then used as an input for ZINDO/SCRF/CV calculation.

Results and Discussions

Comparisons of TPA cross sections obtained from experiment and theory or from two different theoretical methods have many difficulties. Direct comparison of theoretical results with experiment is not possible since (1) spectroscopic measurements of the cross sections have been performed only for a narrow spectral range, and therefore, they do not provide complete information on the TPA line shapes and peak maxima; (2) calculations have been done assuming a uniform empirical broadening parameter $\Gamma = 0.1$ eV for monomers and $\Gamma = 0.15$ eV for aggregates, which is not the case for real molecular systems. Theoretical calculations focus on the maximum limit of the resonant two-photon absorption cross section, which is an intrinsic property of the molecule. When the molecule is placed in a material made of a collection of molecules, the resonance peak gets smaller and broadened. Ahn et al.[12] and Drobizhev et al.[14] have measured the lifetime for porphyrin and its covalently linked dimer, trimer, and tetramer. Collini et al.[10] have measured the lifetime for H_2TPP J-aggregates. All their results show that lifetime decreases from monomer to covalent aggregates or J-aggregates and so Γ should increase with aggregation. For homogeneous broadening to be taken into account, the natural line widths need to be known for our system, and this is seldom the case. To simulate the experimental inhomogeneously broadened absorption profile, one needs to perform summation of the absorption amplitudes over vibrational levels of the first excited electronic state. Unfortunately, for a system with hundreds of vibrational modes, the problem of evaluating the generalized Franck−Condon amplitude is not a trivial one.

TABLE 1: Theoretical Two-Photon Absorption Cross Section (in 10^{-50} cm^4 s/Photon) for H_4TPPS^{2-}, Calculated Using Different Methods and Compared with Available Experimental Values

optimization method	$\langle\delta_{max}\rangle$ calculation method	water $\langle\delta_{max}\rangle$	experimental[a]
HF/6-31G(d,p)/PCM	TD-DFT/PCM	12	
BLYP/6-31G(d,p)/PCM	TD-BLYP/PCM	18	
B3LYP/6-31G(d,p)/PCM	TD-B3LYP/PC	24	30
B3LYP/6-31G(d,p)/PCM	ZINDO/SOS/Onsager	21	
B3LYP/6-31G(d,p)/PCM	ZINDO/CV/Onsager	22	

[a] Experimental values have been obtained from *J. Phys. Chem. B* **2005**, *109*, 2.

Since we do not have actual experimental values, to make a sensible comparison we have used Γ= 0.1 eV for monomer and Γ = 0.15 eV for aggregates. So, this comparison can be used only as a guideline.

To understand the impact of Γ on two-photon absorption properties we have computed the two-photon absorption properties using Γ = 0.08, 0.01, and 0.12 eV for the monomer and Γ = 0.10, 0.15, and 0.2 eV for aggregates. Our results indicate that δ value increases by 1.3 times for monomer as Γ varies from 0.08 to 0.12 ev, whereas δ value increases by 1.6 times for aggregates as Γ varies from 0.10 to 0.2 eV. To calibrate our studies, we have first calculated the TPA cross section of tetrakis(4-sulfonatophenyl) porphyrin diacid (H_4TPPS^{2-}) and have compared this with the TPA cross sections obtained by a different method and by experiments.[10]

We have calculated the TPA properties of H_4TPPS^{2-} and have compared our results with the experimental data (as shown in Table 1) available in the literature. We have optimized the structure by HF, BYLP, and B3LYP methods in the presence of solvents and have calculated the TPA cross section by TD-DFT, TD-HF, and ZINDO/CV method. Our calculation shows that B3LYP method is much better than BLYP or HF method. The TD-B3LYP calculations were carried out using the same basis set and effective core potentials as those used in the ground-state DFT calculations. After optimization, the geometry at the B3LYP level with the 6-31G(d,p) basis set the TD-B3LYP theory was applied for obtaining the excitation energies and transition dipole moments using Gaussian 03 quantum-chemistry code. Frequency-dependent TPA cross section, σ_{TPA}, and the resulting spectra were calculated utilizing 10 excited states and line widths of 0.1 eV with the method recently reported by Badaeva et al.[48] A density matrix formulation of the time-dependent Kohn−Sham equations is used to obtain expressions for the frequency-dependent optical polarizabilities, which are then used to compute the third-order optical response (second-order nonlinear response) and, as a result, σ_{TPA}, as a function of frequency was obtained. To assess the converged character of the TPA values, the frequency-dependent TPA cross section, σ_{TPA}, was calculated utilizing 5, 10, and 15 excited states. Our calculation indicates that δ value increases significantly as we move from 5 to 10 excited states. However, we have noted only a slight increment as we move from 10 to 15 excited states. Our result indicates that δ value calculated using 10 excited states should be near the converged point.

Our calculated ZINDO/CV δ values are in 25% agreement with the experimental value. Though the TD-B3LYP method gave better results than ZINDO/CV method, we have investigated the TPA properties of monomers and aggregates using ZINDO/CV/SCRF method because of following reasons: (1) Prohibitively high computational cost of using the TD-B3LYP/SOS approach for higher aggregates and (2) it has been reported by several publications[49−51] that TD-DFT can overshoot the TPA properties.

SCHEME 2: Structure of Push−Pull Porphyrins Considered in This Paper

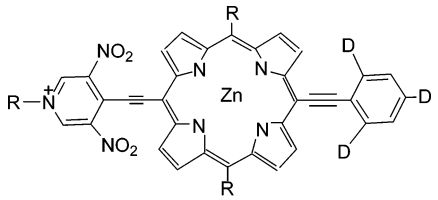

TABLE 2: Theoretical (ZINDO/CV/SCRF) Two-Photon Absorption Wavelength (λ^{TPA} in nm) and Two-Photon Absorption Cross Sections (in 10^{-50} cm^4 s/Photon) and Dipole Moment Change between Ground and Excited States ($\Delta\mu$ in Debye) for Porphyrins with 3,5-Dinitro, *N*-Methyl Pyridinum as an Acceptor and with Different Donors

donor	λ^{TPA}	$\langle\delta_{max}\rangle$	$\langle\Delta\mu\rangle$
NMe_2	1380	8700	45.9
NPh2	1320	9200	51.7
OMe	1280	7200	40.6
Me	1220	6400	32.5
F	1140	5200	26.5

The two-photon absorption maxima shows high red-shift toward desirable wavelengths of (800−1500) nm as the strength of the electron donor increases. Therefore, a well-designed D−A prophyrin system could be an excellent candidate for application in biological imaging and photodynamic therapy. Our results indicate that the TPA cross section increases with the increase in electron donor strength. In fact, the largest TPA cross section obtained, 9200 GM, is comparable with the largest TPA cross section values reported[9] in the literature for organic or organometalic compounds.

The electronic spectra of porphyrin derivatives are usually interpreted using the four-orbital model of Gouterman,[52] which assumes that the HOMO (a_{2u}/a_{1u}) and HOMO−1 (a_{1u}/a_{2u}) of a porphyrin molecule are nearly degenerate, while the LUMO and LUMO−1 (e_g*) are rigorously degenerate. Our calculations indicate that the HOMO and the LUMO of the D−A porphyrin molecules are strongly delocalized, indicating that it is a very good π center. The LUMO of the ZnP compound does not show strong charge separation which probably explains that the first excited state dominated by the HOMO to LUMO transition is not a charge-transfer (CT) state. The first excited state of D−ZnP−A is a strong CT state, possessing both intense one-photon and two-photon absorption cross sections. The HOMO and the LUMO both show very strong charge separation but with opposed signs. In the HOMO, the charge is mainly located on the electron donor side, whereas in the LUMO, it is gathered on the electron acceptor side. To understand the origin of high TPA properties of D−A porphyrins, we have used a two-level model where the TPA cross section can be defined as[22,23]

$$\delta_{2-state} = \frac{4\pi^2 a_0^5 \alpha\omega^2}{15c_0} \frac{M_{ge}^2 \Delta\mu_{ge}^2}{E_{ge}^2 \Gamma} \qquad (5)$$

SCHEME 3: Model Structure of J-Dimer of Porphyrins

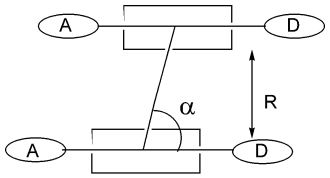

J Aggregate

where a_0 is the Bohr radius, c_0 is the speed of the light, α is the fine structure constant, ω is the photon energy, M_{ge} is the transition dipoles between the ground state $|g>$ and a TPA state $|e>$. $\Delta\mu_{ge}^2$ denotes the square of the change in dipole moment between ground and excited CT states and E_{ge} is the transition energy between the ground state $|g>$ and a TPA state $|e>$. $\Delta\mu_{ge}$ values for all the D−A monomer porphyrins are also reported in Table 2. The results of our calculation indicate that as the charge-transfer character of the ground electronic state increases with increasing donor strength, (1) drastic increase of change in dipole moment between ground and excited CT states occurs; (2) the transition dipole matrix elements $|M_{eg}|$ amplitude increases monotonically; and (3) E_{ge} decreases monotonically.

In case of the dimer, we have taken the optimized monomer structure and have varied only intermolecular distance and the slip angle (the angle between the dipole direction and the line connecting the two centers). We assumed that the two monomers are stacked coplanar with their transition dipoles exactly antiparallel. The interaction between two monomers in the dimer may be understood using the excitonic coupling model[53] as used on the point dipole approximation. According to this model, because of the dipolar interaction, there will be a splitting of the excited energy levels in the magnitude of

$$\Delta E = 2\mu_{DM}^2/4\pi\epsilon_0 R^3(1 - 3\cos^2\alpha)\sin^3\alpha \qquad (6)$$

where μ_{DM} is the transition dipole moment, R is the distance between two monomer centers as shown in Scheme 3, and α is the slip angle. A J-aggregate (as shown in Scheme 3) is formed when the porphyrin molecules arrange into a slanted stack.

The intermolecular interactions are sufficiently strong to significantly change the optical properties of the aggregates compared to the corresponding monomer. Many of the unique properties of the aggregate arise form the fact that the constituent molecules are strongly electronically coupled so that optical excitation of the chromophore produces a state that is delocalized over several monomer units. In addition, excitonic coupling between transient dipoles on neighboring chromophores will split the electronic transition into a broad band of state. This splitting can influence the magnitude of nonlinear optical properties as well as the degree of optical transparency at the wavelengths of interest. The macroscopic photoactive properties such as absorption, emission, and nonlinear optical properties strongly depend on the interaction between the chromophores. To evaluate whether the excitonically coupled monomer model is applicable for porphyrin dimers or not, we carried out ZINDO/CV calculation of the electronic transition energies, oscillator strength of the model dimer for compound 1. For ZINDO/CV calculation, we have used DFT optimized monomer structure at dioxane solvent and then have varied the distance, R, from 3.5 to 8 without changing the monomer geometries. Our results indicate that an excitonically coupled monomer picture is reasonable for interplane separations greater than about 4.46 but breaks down for shorter distances. We cannot neglect totally the orbital overlap between two monomers at the distances of below 4.46. To calculate the TPA properties of J-type dimers in different solvents by ZINDO/CV method, we have used monomer structures optimized in different solvents. We used $R = 4.5$ and slit angle $= 30°$ for J-type dimers, as measured by NMR.[54] Table 3 reports the two-photon absorption maxima of J-type dimers of different D−A porphyrins. The J-dimer shows the expected shift in the absorption to the red with respect to the monomer. The red shift in case of J-dimer is due to the dipolar excitonic coupling between two monomers. The two-photon absorption cross section of J-type dimer is 5−7 times higher than the corresponding monomer. Our results indicate that one can tune the TPA cross section close to an order magnitude with the formation of J-aggregates. Recent experimental[11−14] measurements have shown that the TPA cross sections of the Zn-porphyrin dimer and the Zn-porphyrin tetramer are about 6000 and 8000 GM, respectively. Since the Zn-porphyrin dimer and the Zn-porphyrin tetramer are covalently bonded, this increment can be due to the overlap of molecular orbital. The dimer presented here has excitonic interaction, so we have shown here for the first time that the TPA cross section can be increased to more than 50 000 GM by designing D−A porphyrins excitonic coupling. One of the most promising applications of the gigantic 2PA efficiency of aggregates in the IR region found in this study could be two-photon-induced photodynamic therapy. The fact that the conjugated porphyrin aggregates have such a high two-photon cross section implies that it can have practical applications in high-density optical data storage, 3D fluorescence imaging, and microfabrication.

TABLE 3: Theoretical (ZINDO/CV/SCRF) Two-Photon Absorption Wavelength (λ^{TPA} in nm) and Two-Photon Absorption Cross Section (in 10^{-50} cm^4 s/photon) and Dipole Moment Change between Ground and Excited State ($\Delta\mu$ in Debye) for Porphyrins J-Dimer with 3,5-Dinitro, *N*-Methyl Pyridinum as Acceptor and Different Donors

donor	λ^{TPA}	$\langle\delta_{max}\rangle$	$\langle\Delta\mu\rangle$
NMe_2	1498	47 900	104.6
NPh2	1423	53 000	113.9
OMe	1370	39 000	88.64
Me	1290	34 000	71.6
F	1190	27 000	54.9

To understand the origin of gigantic two-photon absorption properties of the J-aggregates of D−A porphyrins, we have used a two-level model. Our calculations indicate that in the case of J-type dimers, the increment of TPA cross sections is due to three factors, and these are (1) $\Delta\mu_{eg}$ values are about 2.0−2.3 times greater than that of the corresponding monomer, (2) the transition dipole matrix element $|M_{eg}|$ amplitude increases from monomer to dimers, and (3) E_{ge} decreases from monomer to dimers.

Dimers are only a first approximation to the aggregates present in real materials. In a real chromophore−polymer system at higher chromophore loading, the chromophore may exist in a wide range of forms including monomers, various types of dimers, higher aggregates, and large nano- or microcrystalline states. So, it is very important to understand how the TPA cross section values vary with the increase in the number of monomers in both J-aggregates. In case of higher aggregates, we have taken DFT optimized monomer structure using solvent dielectric constant, as the optimized structure and the monomers are separated by 4.5 to each other. The slit angle is kept as 30° for J-type aggregates. Figure 1 shows how the two-photon absorption cross section changes with the number of monomers in the aggregates. Our calculations indicate that the δ values for J-type aggregates increase tremendously, about 50−70 times

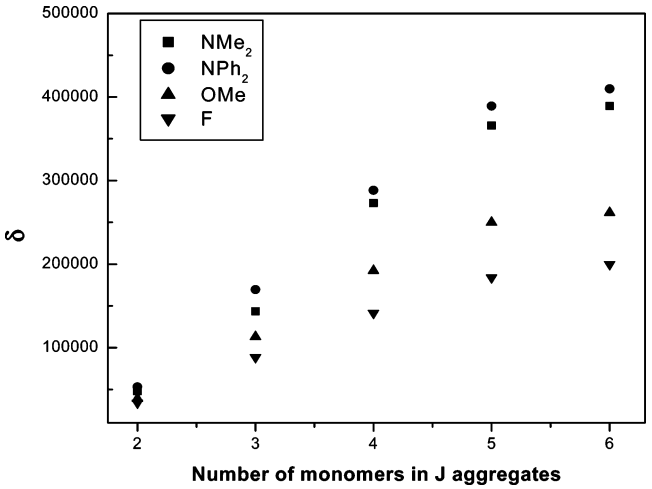

Figure 1. Plot of δ (in 10^{-50} cm^4 s/photon) vs number of monomers in the J-type aggregates for porphyrins with 3,5-dinitro, *N*-methyl pyridinum as an acceptor and different donors.

from monomer to pentamer and then approaches saturation. This can explain the recent experimental observation[10] of strong enhancement of TPA cross section of tetrakis(4-sulfonatophenyl)porphyrin diacid in water solvent. They have reported 30-fold enhancement of the TPA cross section values upon aggregation. To understand the origin of very high two-photon absorption properties of higher J-aggregates, we have performed calculations of $\Delta\mu_{eg}$ and $|M_{eg}|$. Our calculations indicate that both $\Delta\mu_{eg}$ values and transition dipole matrix element $|M_{eg}|$ amplitude increase with the increasing number of monomers in aggregates till pentamer and then become near saturation, whereas E_{ge} decreases monotonically till pentamer and then become near saturation.

Conclusion

In this paper, we have reported for the first time the TPA properties of aggregates of push−pull porphyrin chromophores. We have analyzed a variety of effects on the TPA properties for porphyrin monomers and aggregates. We have designed a series of D−A Zn-porphyrin derivatives that possess exceptionally large TPA cross sections at the desirable fundamental wavelengths of 1.1−1.5 m, which can be highly suitable candidates for the applications in biological imaging and photon dynamic therapy. The evolution of the CT state with respect to the electron donor/acceptor substitutions has been discussed. Our results indicate that for D−A porphyrin system, as the donor strength increases, (1) change of dipole moment between ground and excited CT states increases tremendously, (2) the transition dipole matrix element $|M_{ge}|$ amplitude monotonically increases, and (3) E_{ge} decreases monotonically. We have demonstrated that the TPA cross section values of J-type aggregates are 50−70 folds higher than that of monomers and it is because (1) $\Delta\mu_{eg}$ values for higher aggregates are about 5−7 times higher than that of the corresponding monomer and (2) the transition dipole matrix element $|M_{eg}|$ amplitude increases and (3) E_{ge} decreases monotonically. The large enhancement of two-photon absorption in aggregates has potential for application in imaging and localized activation of photochemical processes. An important consequence of the extremely high TPA cross section will allow the use of very low laser intensity to produce a given fluorescence signal, which can be of significance in biological applications. We believe that push−pull porphyrin aggregates are interesting systems with potential to increase the impact of two-photon processes in photonics, materials processing, chemical sensing, and biological applications.

Acknowledgment. We thank the NSF-PREM Grant #DMR-0611539 for generous funding. We also thank Mississippi Center for Super Computer Resource (MCSR), University of Mississippi, Oxford, MS, for the generous use of their computational facilities. We also thank reviewers whose valuable suggestions improved the quality of the manuscript.

References and Notes

(1) Drobizhev, M.; Stepanenko, Y.; Dzenis, Y.; Karotki, A.; Rebane, A.; Taylor, P. N.; Anderson, H. L. *J. Am. Chem. Soc.* **2004**, *126*, 15352−15353.

(2) Ahn, T. K.; Kim, K. S.; Kim, D. Y.; Noh, S. B.; Aratani, N.; Ikeda, C.; Osuka, A.; Kim, D. *J. Am. Chem. Soc.* **2006**, *128*, 1700−1704.

(3) Woo, H. Y.; Liu, B.; Kohler, B.; Korystov, D.; Mikhailovsky, A.; Bazan, G. C. *J. Am. Chem. Soc.* **2005**, *127*, 14721.

(4) Bartholomew, G. P.; Rumi, M.; Pond, S. J. K.; Perry, J. W.; Tretiak, S.; Bazan, G. C. *J. Am. Chem. Soc.* **2004**, *126*, 11529−11542.

(5) Pati, S. K.; Marks, T. J.; Ratner, M. A. *J. Am. Chem. Soc.* **2001**, *123*, 7287−7291.

(6) Beverina, L.; Fu, J.; Leclercq, A.; Zojer, E.; Pacher, P.; Barlow, S.; Van Stryland, E. W.; Hagan, D. J.; Bredas, J.-L.; Marder, S. R. *J. Am. Chem. Soc.* **2005**, *127*, 7282.

(7) Chung, S.-J.; Rumi, M.; Alain, V.; Barlow, S.; Perry, J. W.; Marder, S. R. *J. Am. Chem. Soc.* **2005**, *127*, 10844.

(8) Humphrey, J. L.; Kuciauskas, D. *J. Am. Chem. Soc.* **2006**, *128*, 3902.

(9) Das, S.; Nag, A.; Goswami, D.; Bharadwaj, P. K. *J. Am. Chem. Soc.* **2006**, *128*, 402.

(10) Collini, E.; Ferrante, C.; Bozio, R. *J. Phys. Chem. B* **2005**, *109*, 2−5.

(11) Kim, D. Y.; Ahn, T. K.; Kwon, J. H.; Kim, D.; Ikeue, T.; Aratani, N.; Osuka, A.; Shigeiwa, M.; Maeda, S. *J. Phys. Chem. A.* **2005**, *109*, 2996−2999.

(12) Ahn, T. K.; Kwon, J. H.; Kim, D. Y.; Cho, D. W.; Jeong, D. H.; Kim, S. K.; Suzuki, M.; Shimizu, S.; Osuka, A.; Kim, D. *J. Am. Chem. Soc.* **2005**, *127*, 12856−12861.

(13) Ogawa, K.; Ohashi, A.; Kobuke, Y.; Kamada, K.; Ohta, K. *J. Phys. Chem. B* **2005**, *109*, 22003−22012.

(14) Drobizhev, M.; Stepanenko, Y.; Dzenis, Y.; Karotki, A.; Rebane, A.; Taylor, P. N.; Anderson, H. L. *J. Phys. Chem. B* **2005**, *109*, 7223−7236.

(15) Woo, H. Y.; Korystov, D.; Mikhailovsky, A.; Nguyen, T.-Q.; Bazan, G. C. *J. Am. Chem. Soc.* **2005**, *127*, 13794−13795.

(16) Ogawa, K.; Ohashi, A.; Kobuke, Y.; Kamada, K.; Ohta, K. *J. Am. Chem. Soc.* **2003**.

(17) Zheng, Q.; He, G. S.; Prasad, P. N. *Chem. Mater.* **2005**, *17*, 6004−6011.

(18) Wang, Y.; He, G. S.; Prasad, P. N.; Goodson, T., III. *J. Am. Chem. Soc.* **2005**, *127*, 10128−10129.

(19) Albota, M.; et al. *Science* **1998**, *281*, 1653−1650.

(20) Ray, P. C.; Leszczynski, J. *J. Phys. Chem. A* **2005**, *109*, 6689−6696.

(21) Zhou, X.; Ren, A.-M.; Feng, J.-K.; Liu, X.-J.; Zhang, Y.-D. *Chem. Phys. Chem.* **2003**, *4*, 991−997.

(22) Luo, Y.; Oscar, R.-P.; Guo, J.-D.; Agren, H. *J. Chem. Phys.* **2005**, *122*, 96101.

(23) Oscar, R.-P.; Agren, H. *J. Chem. Phys.* **2006**, *124*, in press.

(24) Masunov, A.; Tretiak, S. *J. Phys. Chem. B* **2004**, *108*, 899−907.

(25) Clark, A. E. *J. Phys. Chem. A* **2006**, in press

(26) Zalesny, R.; Bartkowiak, W.; Styrcz, S.; Leszczynski, J. *J. Phys. Chem. A* **2002**, *106*, 4032−4037.

(27) Van Stryland, E. W.; Wu, Y. Y, Hagan. D. J.; Soileau, M. J.; Mansour, K. *J. Opt. Soc. Am. B* **1988**, *5*, 1980.

(28) Mukherjee, A. *Appl. Phys. Lett.* **1993**, *62*, 3423.

(29) Wang, X.; Kerbs, L. J.; Pudavar, H. E.; Ghosal, S.; Liebow, C.; Schally, A. V.; Prasad, P. N. *Proc. Natl. Acad. Sci. U.S.A.* **1999**, *96*, 11081.

(30) Joshi, M. P.; Pudavar, H. E.; Swaitkiewicz. J; Prasad, P. N.; Reianhardt, B. *Appl. Phys. Lett.* **1999**, *74*, 170.

(31) Kawatta, S.; Kawatta, Y. *Chem. Rev.* **2000**, *100*, 1777.

(32) Ogawa, K.; Hasegawa, H.; Inaba, Y.; Kobuke, Y.; Inouye, H.; Kanemitsu, Y.; Kohno, E.; Hirano, T.; Ogura, S.-i.; Okura, I. *J. Med. Chem.* **2006**, in press.

(33) Bhawalkar, J. D.; Kumar, N. D.; Zhao, C. F.; Prasad, P. N. *J. Clin. Laser, Med. Surg.* **1997**, *15*, 201.

(34) Bauer, C.; Schnabel, B.; Kley, E. B.; Scherf, U.; Giessen, H.; Mahrt, R. F. *Adv. Mater.* **2002**, *14*, 673.

(35) Spangler, C. W. *J. Mater. Chem.* **1999**, *9*, 2013.

(36) Ramasesha, S.; Shuai, Z.; Bredas, J. L. *Chem. Phys. Lett.* **1995**, *245*, 226.

(37) Ray, P. C.; Ramasesha, S.; Das, P. K. *J. Chem. Phys.* **1996**, *105*, 9633.
(38) Ray, P. C. *Chem. Phys. Lett.* **2004**, *394*, 354.
(39) Ray, P. C. *Chem. Phys. Lett.* **2004**, *395*, 269.
(40) Ray, P. C.; Leszcynski, J. *Chem. Phys. Lett.* **2004**, *399*, 162.
(41) Sainuideen, Z.; Ray P. C. *J. Phys. Chem. A* **2005**, *109*, 9095.
(42) Ray, P. C.; Leszczynski, J. *Chem. Phys. Lett.* **2006**, *419*, 578.
(43) Jha, P. C.; Das, J. M.; Ramasesha, S. *J. Phys. Chem. A* **2004**, *108*, 6279.
(44) Tomasi, J.; Mennucci, B.; Cammi.; R. *Chem. Rev.* **2005**, *105*, 2999.
(45) Onsager, L. *J. Am. Chem. Soc*. **1936**, *58*, 1486.
(46) Frisch, M. J.; Trucks, G. W.; Schlegel, H. B.; Scuseria, G. E.; Robb, M. A.; Cheeseman, J. R.; Montgomery, J. A., Jr.; Vreven, T.; Kudin, K. N.; Burant, J. C.; Millam, J. M.; Iyengar, S. S.; Tomasi, J.; Barone, V.; Mennucci, B.; Cossi, M.; Scalmani, G.; Rega, N.; Petersson, G. A.; Nakatsuji, H.; Hada, M.; Ehara, M.; Toyota, K.; Fukuda, R.; Hasegawa, J.; Ishida, M.; Nakajima, T.; Honda, Y.; Kitao, O.; Nakai, H.; Klene, M.; Li, X.; Knox, J. E.; Hratchian, H. P.; Cross, J. B.; Bakken, V.; Adamo, C.; Jaramillo, J.; Gomperts, R.; Stratmann, R. E.; Yazyev, O.; Austin, A. J.; Cammi, R.; Pomelli, C.; Ochterski, J. W.; Ayala, P. Y.; Morokuma, K.; Voth, G. A.; Salvador, P.; Dannenberg, J. J.; Zakrzewski, V. G.; Dapprich, S.; Daniels, A. D.; Strain, M. C.; Farkas, O.; Malick, D. K.; Rabuck, A. D.; Raghavachari, K.; Foresman, J. B.; Ortiz, J. V.; Cui, Q.; Baboul, A. G.; Clifford, S.; Cioslowski, J.; Stefanov, B. B.; Liu, G.; Liashenko, A.; Piskorz, P.; Komaromi, I.; Martin, R. L.; Fox, D. J.; Keith, T.; Al-Laham, M. A.; Peng, C. Y.; Nanayakkara, A.; Challacombe, M.; Gill, P. M. W.; Johnson, B.; Chen, W.; Wong, M. W.; Gonzalez, C.; Pople, J. A. *Gaussian 03*, revision A.11; Gaussian, Inc.: Pittsburgh, PA, 2003.
(47) Setvens, W. J.; Basch, H.; Krauss, M. J. *J. Chem. Phys.* **1984**, *81*, 6027.
(48) Badaeva, E. A.; Timofeeva, T. V.; Masunov, A.; Tretiak, S. *J. Phys. Chem. A* **2005**, *109*, 7276.
(49) Dreuw, A.; Gordon, M. H. *J. Am. Chem. Soc*. **2000**, *104*, 4755.
(50) Champagne, B.; Perpte, E. A.; Jacquemin, D.; Van Gisbergen, S J. A.; Baerends, E.-J.; Soubra-Ghaoui, C.; Robins, K. A.; Kirtman, B. *J. Phys. Chem. A* **2000**, *104*, 4755.
(51) Tozer, D. J. *J. Chem. Phys.* **2003**, *119*, 12697.
(52) Gouterman, M. *J. Mol. Spectrosc.* **1961**, *6*, 138−163.
(53) Mccullough, J. *Chem. Rev.* **1987**, *87*, 811.
(54) Koji, K.; Kazuya, F.; Hideo, W.; Ryuhei, N.; Robert, P. F. *J. Am. Chem. Soc.* **2000**, *122*, 7494.